Developing Surrogates for Liquid Transportation Fuels: The Role of Spherically Symmetric Droplet Combustion

C. Thomas Avedisian

Abstract The finite supply of transportation fuels has generated renewed interest to improve their performance in power and propulsion devices. However, the complexity of real fuels prohibits developing their combustion chemistries and property databases needed for simulating performance in engines to identify operational regimes for improving fuel efficiency. Surrogates offer the means to address these concerns if they can be shown to replicate certain combustion targets of the real fuel, and to result in combustion properties similar to real fuels when burned in a suitable configuration that is amenable to detailed numerical modeling. This paper examines the role which droplet combustion can play in the development of surrogates for complex transportation fuels. Recognizing that spray combustion is far too difficult to model and that droplets represent the fine-grid structure of sprays, the combustion dynamics of fuel droplets are examined in an environment that seeks to remove external convective influences to simplify the transport field and produce spherical symmetry in the droplet burning process that can be modeled using a detailed numerical simulation approach. The one-dimensional flames and transport dynamics that result are shown to be well positioned to evaluate the efficacy of surrogate fuel performance. Recent efforts are summarized that have used the spherical droplet flame configuration to evaluate the performance of surrogate fuel blends. Experiments are discussed for promoting spherical symmetry, and results are presented to show the efficacy of some surrogate blends to replicate the performance of gasoline and jet fuels using the spherical droplet configuration. Some results are also included from detailed numerical modeling of biodiesel droplets that incorporate complex combustion chemistry, and unsteady transport, vaporization, and variable property effects that illustrate the potential for high fidelity predictions needed for developing surrogates using the spherically symmetric droplet flame configuration.

This paper is based on a presentation given at the Indo-US International Workshop on Novel Combustion for Sustainable Energy Development, Kanpur, India, January 2–4, 2014.

C.T. Avedisian (✉)
Sibley School of Mechanical and Aerospace Engineering, Cornell University,
Ithaca, NY 14853-7501, USA
e-mail: cta2@cornell.edu

A.K. Agarwal et al. (eds.), *Novel Combustion Concepts for Sustainable Energy Development*, DOI 10.1007/978-81-322-2211-8_16

Keywords In-cylinder combustion · Surrogate fuels · Low-dimensional combustion · Fuel spray · Multiphase processes

1 Introduction

In 2013, almost 90 million barrels of liquid fuels were consumed in power and propulsion devices worldwide. The United States was the largest consumer at 20 % (USEIA 2014). The transportation sector accounted for approximately 70 % of this consumption. The emissions produced, and the fact that much of the oil used is imported, has motivated investments in alternative propulsion and energy technologies (e.g., electric, wind, solar, geothermal) that would also reduce reliance on foreign supplies. However, these alternatives are not yet at the stage to significantly impact petroleum use or fully meet the transportation and energy needs of modern societies (NSF 2011). And none of them currently matches the cost and energy density of liquid fuels. Biofuels derived from nonfood feedstocks have generated significant interest to complement, and eventually replace, petroleum-based fuels. There are, however, issues that need to be resolved for them to realize their full potential as an alternative to petroleum fuels (Dirks et al. 2012). Nonetheless, the need for liquid fuels is expected to remain even as the supply of petroleum-based fuels is limited (NSF 2011).

Internal combustion and aircraft engines are the primary consumers of liquid fuels. A further stimulus for improving engine efficiency comes from new regulations (i.e., in the U.S.) for the ground transportation sector that mandate fuel economy levels of 54.5 miles per gallon by 2025 for new model cars as shown in Fig. 1 (FR 2012). As such, development of technologies that improve the efficiency

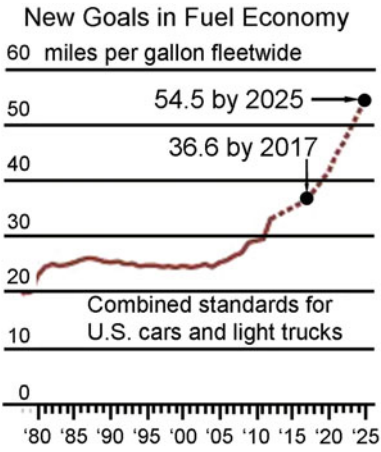

Fig. 1 New fuel economy targets for 2025 (FR 2012)

of combustion engines stands to have an immediate impact on petroleum fuel supplies and their clean combustion.

Considering the design process for bringing new engine technologies to the marketplace, experimental testing and prototype evaluation have been the standard approach of the transportation sector. The emergence of powerful computational capabilities is beginning to change this paradigm. For example, the Cummins ISB 6.7 l diesel was developed entirely by computer simulation (PRECISE 2011), with the only testing coming from performance evaluation after prototype fabrication and operation. The new engine also achieved mileage targets and emission constraints of the design.

The prediction of in-cylinder processes is a challenging task owing to the difficulty of incorporating all of the relevant physics for engine processes in a first-principles solver. The presence of liquid droplets associated with spray injection and the combustion chemistry that provides the chemical pathways for oxidation of the fuel are particularly problematic. Sub-model inputs and approximations are typically needed to enable predictions of performance. For example, the often used KIVA code (Amsden 1999; Lee and Reitz 2013) requires sub-models for soot and the real fuel combustion chemistry, the phase equilibrium (distillation) characteristics of the fuel, adjustable parameters to make the spray liquid and vapor penetrations match experimental data and values of the crank angle where 10 % of the fuel is burned (Wang et al. 2013), thermofluid properties, turbulence, droplet collision dynamics, and evaporation for multicomponent droplets.

The context of the challenges involved with predicting the performance of engines powered by real transportation fuels is illustrated by considering their compositions. Real petroleum-based fuels—gasoline, jet, diesel—consist of hundreds of miscible constituents with a wide range of volatilities, sooting propensities, and thermo-physical properties. Table 1 lists broad chemical classes present in a typical jet fuel (i.e., Jet A is basically JP8 minus additives for lubricity, de-icing, and antistatic effects (Edwards and Maurice 2001), and Table 2 lists the major components for diesel.

Figure 2 illustrates the mole percents of the broad chemical classes' hydrocarbons in a typical gasoline blend (Tsang 2003). The highly multicomponent nature of real fuels is further complicated by the variability of manufacturing, with

Table 1 Constituents of a typical Jet A fuel (Colket et al. 2007)

Component	(v %)
Paraffins	55.2
Monoclycloparaffins	17.2
Dicycloparaffins	7.8
Tricycloparaffins	0.6
Alkyl benzenes	12.7
Indans + tetralins	4.9
Naphthalene	<0.2
Substituted naphthalenes	1.3

Table 2 Typical diesel fuel components (Farrell et al. 2007)

Component	(v %)
Normal and isoparaffins	25–50
Cyclo-paraffins	20–40
Aromatics	15–40

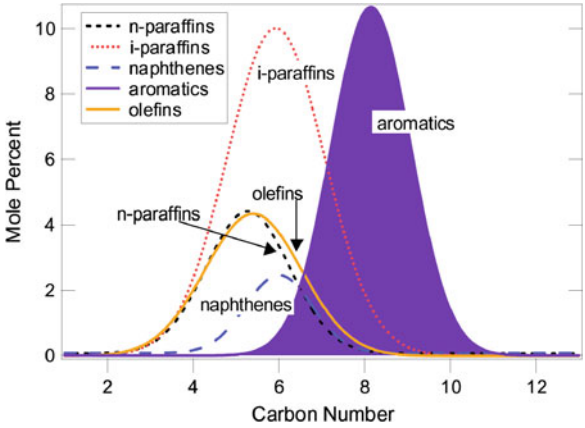

Fig. 2 Typical gasoline composition showing concentration by chemical classes (adapted from Tsang 2003)

compositions that can vary depending on the nature of the crude, time of year, and the refinery (Farrell et al. 2007). The result is that fuels produced from different production runs or refineries may not have precisely the same properties.

The multicomponent characteristic of real fuels makes it a significant challenge to develop the required inputs for simulation, including predicting the phase equilibrium behavior, properties, and combustion kinetics as noted above. The problem is further exacerbated by the new generation of biofuels about which much effort has been devoted to production but little to evaluating combustion performance.

The only viable approach to simulating combustion performance of real fuels in engines is to develop a "surrogate" for them. A surrogate is defined as a blend of relatively fewer compounds of known chemical species and mixture fractions which are selected to match certain thermochemical aspects ("targets")[1] of the real fuel (Dooley et al. 2010, 2012; Liu and Avedisian 2012; Zhang et al. 2007; Mueller et al. 2012; Narayanaswamy et al. 2013; Pitz and Mueller 2011). With appropriate blending and mixing strategies, the surrogate may replicate most (but often not all) of the combustion targets around which it is developed. It is advantageous that the number of constituents of the surrogate blend should be as low as possible in order to make tractable the prediction of properties and phase equilibrium behavior, as well as to develop combustion chemistry. The simplest surrogate would be a single

[1] A combustion "target" is defined here as a variable used for matching a surrogate with a real fuel (e.g., molecular weight, derived cetane number, liquid density). A combustion "property" is defined as a variable measured in a combustion configuration.

component hydrocarbon (e.g., n-heptane = #2 diesel fuel (Wang et al. 2013) or combining the kinetic mechanism of methyl butanoate with heptane for a soybean biodiesel (Lee et al. 2013).

A step-up from a single component hydrocarbon is a binary blend which have been used as surrogates (i.e., a n-dodecane/iso-octane = a multicomponent paraffinic jet fuel in a specific mixture (mole) fraction of [i.e., 0.519/0.481 (Dooley et al. 2012)]). Three and four component blends have been successfully developed for some transportation fuels (Dooley et al. 2010, 2012). Higher-order surrogates have been formulated with eight components to represent a certification gasoline and reference diesel fuel (Mueller et al. 2012). It is clearly advantageous to have a surrogate with as few components as possible to enable predictions of physical and thermodynamic properties with minimal effort.

This paper reviews the development of surrogates from the perspective of liquid fuels and the role that droplet combustion dynamics can play in this process. Experimental results are presented that show the efficacy of a simplified droplet burning configuration for evaluating the performance of gasoline and jet fuel. Some results related to detailed numerical simulation of droplet combustion of biofuel surrogates are also included.

2 The Canonical Configuration for Liquid Fuel Combustion

Developing a surrogate involves several tasks: (1) determining the broad chemical classes of the real fuel; (2) selecting the surrogate components; (3) calculating the fractional amounts of the surrogate components through a process that minimizes the difference between selected combustion targets of the surrogate and real fuel (e.g., by various optimization methods (Narayanaswamy et al. 2013; Dooley et al. 2010, 2012)); (4) comparing combustion properties of the surrogate to the real fuel as measured in a suitable combustion configuration; and (5) assessing the efficacy of the surrogate to produce high fidelity predictions of combustion properties measured in a suitable combustion configuration.

Considering combustion properties pertinent to liquid fuels, at one extreme is the stochastic environment of a piston engine (Fig. 3), with its swirling and turbulent motion, spray dynamics, and radiation.

Ab initio models for engines do not exist. The KIVA code (Amsden 1999) is one of the more advanced solvers of the transport equations for in-cylinder combustion dynamics that includes models for spray injection. Nonetheless, detailed numerical modeling of spray combustion is also beyond current capabilities (i.e., when including, simultaneously, detailed combustion kinetics, radiative and unsteady effects, droplet formation, evaporation). This leaves processes at the level of individual droplets to consider. Here too, there are significant challenges.

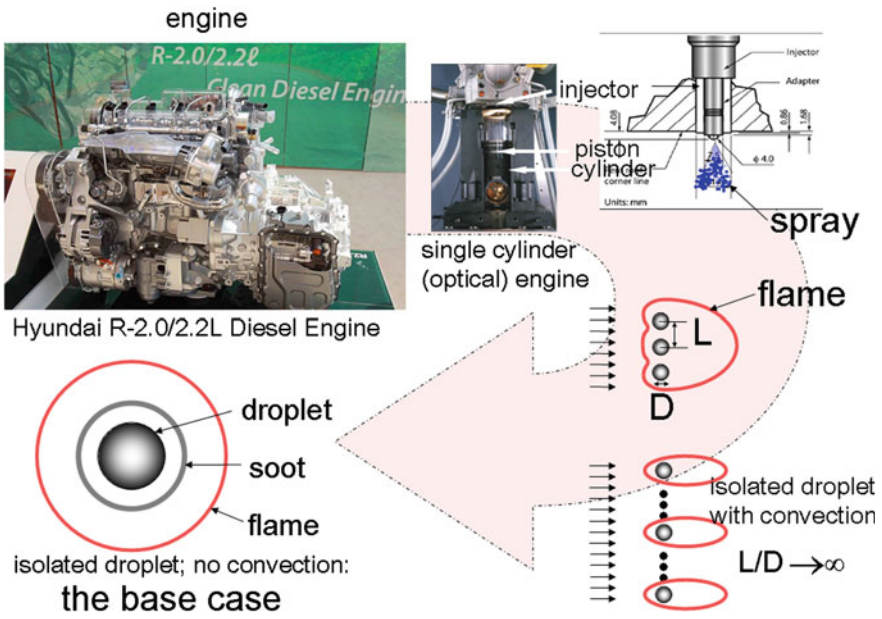

Fig. 3 Context of the spherically symmetric droplet burning configuration to the stochastic environment of an engine

A hierarchy for combustion of a liquid fuel is envisioned as depicted in Fig. 3 that includes a full spray, 3-D multi-droplet cloud, and 2-D array with inter-droplet spacing "L". For finite L, none of these configurations is yet amenable to ab initio modeling that includes simultaneously the effects of time-dependent gas and liquid transport, moving boundary of the liquid/gas interface as evaporation occurs, variable properties, detailed combustion chemistry, and radiation. Even if L is arbitrarily "large" such that a single isolated drop is realized but convective effects are still present, detailed numerical simulation has not yet been accomplished, though approaches have included some (but not all) of these elements (Sirignano 1999).

Currently, it appears that only for the single stationary isolated droplet ($L \rightarrow \infty$ in Fig. 3), burning in a quiescent ambience with no convective effects (forced or buoyancy-induced) can detail numerical simulation based on a first-principles solution be carried out that incorporates all the physical processes mentioned above, except for soot formation (Farouk et al. 2013, Liu et al. 2013a; Cuoci et al. 2005). Figure 4a is a schematic of this configuration.

The gas flow will be one-dimensional and only in the radial direction, and the flow is created entirely by the evaporation process. If soot forms [Fig. 4b, c (Liu et al. 2014a)], the soot aggregates will be trapped between the droplet and flame by the forces acting on the particles (Avedisian 1997). The configuration of Fig. 4 represents the "base case" of liquid fuel combustion as a building block for complex droplet configurations that lead to spray dynamics.

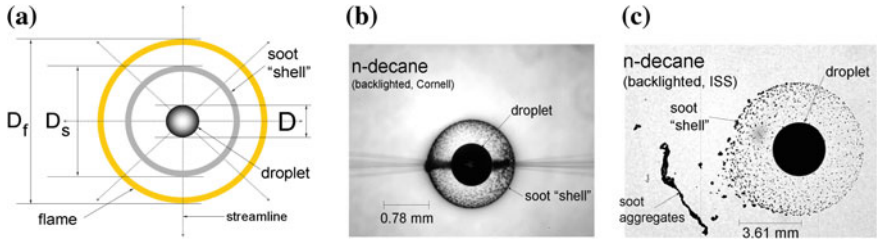

Fig. 4 **a** Schematic representation of an isolated droplet burning with spherical symmetry. **b** Backlighted photograph of a "small" fiber-supported n-decane droplet burning in the standard atmosphere at normal atmospheric pressure and showing the soot shell; **c** "large" free or unsupported n-decane droplet burning in the MDCA of the International Space Station in the standard atmosphere

The attractiveness of a low-dimensional transport configuration for developing surrogates has been recognized. The principle advantage is that detailed numerical modeling can be applied, thereby allowing a rigorous test of the combustion kinetics. For example, configurations have included shock tubes and rapid compression machines (Gauthier et al. 2004; Yahyaoui et al. 2007; Werler et al. 2014), counter flow flames and jet-stirred reactors (Choi et al. 2011; Dagaut et al. 2008), and premixed and non-premixed flow reactors (Chaos et al. 2007; Bieleveld et al. 2009), among others. They require that the fuel be pre-vaporized before entering the combustion zone. Pre-vaporization eliminates the intimate relationship between fuel vaporization and multicomponent effects for sustaining the flame that is intrinsic to the combustion of sprays and droplets in engines.

With liquid fuel injection comes evaporation and moving boundary effects; the configuration of Fig. 4 incorporates these processes. Phase equilibrium of the fuel determines the evaporation rate of liquid in a spray; and the temperature of an isolated droplet is also controlled by this process. Unsteady gas and liquid transport, soot formation, and radiation are intrinsic to in-cylinder processes in which the configuration of Fig. 4 also includes. The isolated droplet case incorporates these aspects as a natural consequence of the burning process. There is also carryover of such aspects as soot morphology and combustion chemistry of the base case of Fig. 4 to the more complex conditions of an engine. As such, the combustion symmetry of an isolated droplet burning with no convective effects is considered to be an appropriate platform for developing combustion properties for developing surrogate fuels.

It is also worth-mentioning that developing surrogates from the perspective of individual droplets is attractive for the very small liquid volumes needed for droplet combustion experimentation. In spray or engine tests, tens of gallons are typically required to evaluate performance. New fuel blends can be in short supply (e.g., algal biodiesel) with the availability of a sufficient fuel supply limiting the range of conditions that can be evaluated in experiments. On the other hand, droplet combustion experiments utilize very small volumes, on the order of 10^{-8} gallons per burning event, and will not be restricted by this concern.

The configuration of Fig. 4 is obviously not the same as the stochastic environment of an engine, though it does serve as a building block for a progression of complexities that lead to relevance to an engine environment. Even for the configuration of Fig. 4, the same basic mechanisms of combustion present in an engine exist in the spherical droplet flame configuration. Its greatest virtue for developing surrogate fuels is that it is amenable to detailed numerical modeling (Liu et al. 2013a; Farouk et al. 2013; Fahd et al. 2014) which allows for a more rigorous test of the surrogate fuel chemical kinetics with combustion properties that include vaporization and liquid-phase multicomponent effects. For these reasons, the isolated droplet burning geometry can be viewed as a canonical configuration for liquid fuel combustion.

3 Developing a Surrogate for Liquid Transportation Fuels

Surrogate components are selected with reference to broad chemical classes of the real fuel (Dooley et al. 2010, 2012; Huber et al. 2010; Mueller et al. 2012; Narayanaswamy et al. 2013). Once identified, their fractional amounts need to be determined. A simple approach involves sweeping through compositions to identify ones where the real and surrogate fuel targets match. This primitive approach looses its appeal for more than one target or binary system (Avedisian 2008).

For a general multicomponent surrogate, constrained optimization or regression techniques are used to identify the fractional amounts that reduce the difference between the real and surrogate fuel targets (Dooley et al. 2010, 2012; Narayanaswamy et al. 2013; Mueller et al. 2012; Huber et al. 2010). There is no universal set of targets for developing a surrogate. They are linked to the application (Pitz et al. 2007). Targets that have been considered for transportation fuels include various combinations of the hydrogen-to-carbon (H/C) ratio, derived cetane number (DCN), threshold sooting index (TSI), average molecular weight (MW_{ave}), liquid density, and advanced distillation curve to characterize the phase behavior of the fuel. Typically, four targets are involved in the matching process.

In the next sections, we discuss the performance of several surrogates for liquid transportation fuels from the perspective of the spherical droplet flame configuration. We begin with a brief discussion of the experimental designs for creating near-spherically symmetric droplet burning conditions. We then present some experimental results and include discussion of the performance of a surrogate developed using the optimization process mentioned above. Some results are also discussed for detailed numerical modeling of the spherical droplet flame configuration for a biodiesel surrogate.

4 Creating Spherically Symmetric Droplet Burning Conditions

The computational simplicity of the one-dimensional droplet flame in Fig. 4 belies the experimental difficulty of creating this configuration; it is arguably the most difficult combustion configuration to create in all of combustion science. To create spherically symmetric droplet burning conditions, an environment is required where the dynamic parameters that control convection are "small": The Rayleigh number $\left(Ra = \frac{g\beta\Delta TD^3}{\alpha\nu}\right)$ and Reynolds number $\left(\mathrm{Re} = \frac{UD}{\nu}\right)$ are most relevant, where g, β, ΔT, D, ⍺ U_∞, and ν are gravity, thermal expansion coefficient, characteristic temperature difference (e.g., flame and droplet temperatures), droplet diameter, gas thermal diffusivity, relative velocity between the droplet and surrounding gas, and kinematic viscosity, respectively (D_f may also be used as the characteristic dimension though it is related to the droplet diameter). It is seen that there are a number of ways that convective influences on the burning process can be reduced. The gravitational level is typically reduced to promote a small Ra, while various experimental configurations are designed to form, deploy, and ignite the droplet with minimal disturbances and residual droplet motion to make Re suitable small.

Reduced gravity is created by performing the experiments in a free fall facility, either on Earth over a distance that determines the experimental time [i.e., a drop tower (Avedisian et al. 1988)] or in an orbiting craft [e.g., the International Space Station (ISS) (Dietrich et al. 2014)] which is essentially in free fall as it orbits the Earth.

The experimental design must form, deploy, and ignite the test droplet without any significant accompanying motion to these operations. The droplet can either be physically restricted by some sort of a support fiber attached to the droplet (Avedisian and Jackson 2000) or free of any support structures that do not impart any residual motion to the droplet during the deployment process (Avedisian et al. 1988; Okajima and Kumagai 1975; Hara and Kumagai 1990; Liu et al. 2014b; Avedisian and Callahan 2000; Jackson et al. 1991).

The experimental designs are broadly tailored to "small" droplets corresponding to initial diameters (D_o) of $D_o < 1$ mm and "large" droplets corresponding to $D_o > 1.5$ mm. Small droplet experiments are most suitable for experimental times on the order of several seconds (i.e., as in drop towers). Large droplet experiments will typically require several tens of seconds to observe the complete droplet burning history and are best examined in the environment of the ISS where the experimental time is unlimited.

For small droplets, radiative effects are not important. For large droplets, radiation can be important to promote extinction with the possibility of "cool flames" (Nayagam et al. 2012; Farouk and Dryer 2013; Dietrich et al. 2014) that are characterized by a low-temperature combustion regime of burning. By varying D_o from about 0.5 mm up to about 6 mm, the complete range of physical phenomenon a liquid fuel could experience in a combustion environment can be accessed.

A small droplet experimental configuration is schematically shown in Fig. 5. It involves deploying a test droplet at the vertex of two very small diameter fibers crossed at an angle, essentially by propelling the test droplet onto the vertex with a droplet generator (i.e., it is very difficult to deploy a droplet on the order of 0.5 mm onto a 14-μm-diameter support structure by other methods). At that point, and after the period of free fall begins, the droplet is then ignited by two sparks positioned on opposite sides of the droplet to provide some degree of symmetry to the ignition process. Digital video cameras record the burning history.

An unsupported droplet can be created using this same basic approach by essentially removing the crossed fibers but still retaining the droplet trajectory. At the apex of the trajectory, cameras positioned there, along with the sealed gas in which the deployment process is carried out, are then literally released into free fall (Okajima and Kumagai 1975; Avedisian et al. 1988). The downward motion of the droplet falling at the same rate as the imaging system then creates the illusion of a levitated droplet. Though creating unsupported droplets is very difficult, if successful images like those shown in Fig. 4b and c will result.

For large droplets, the multiuser droplet combustion apparatus (MDCA) is designed to form and deploy unsupported or free-floating droplets using the approach schematically illustrated in Fig. 6 (Banu 2008; Robbins and Shinn 2010, and Dietrich et al. 2014).

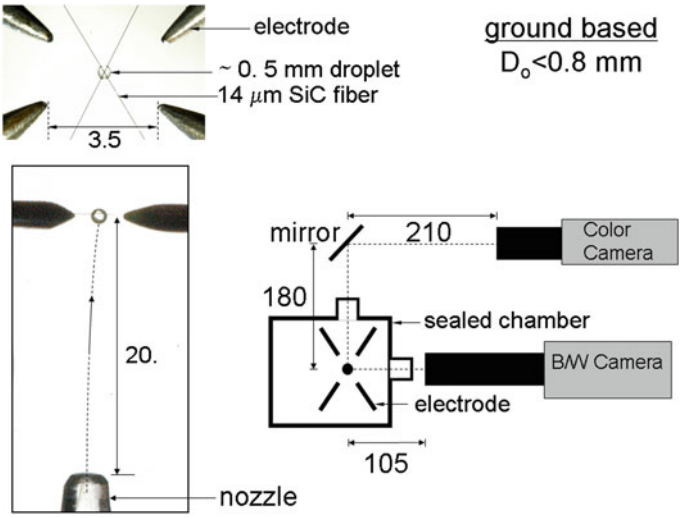

Fig. 5 Droplet deployment design for ground-based experiments (Liu et al. 2012). Numbers are in millimeters. Camera arrangement for recording the droplet burning history is shown. To create an unsupported droplet, the 14-μm fiber is removed and the sealed chamber is released into free fall when the droplet reaches the apex of its approximately 20 mm deployment trajectory

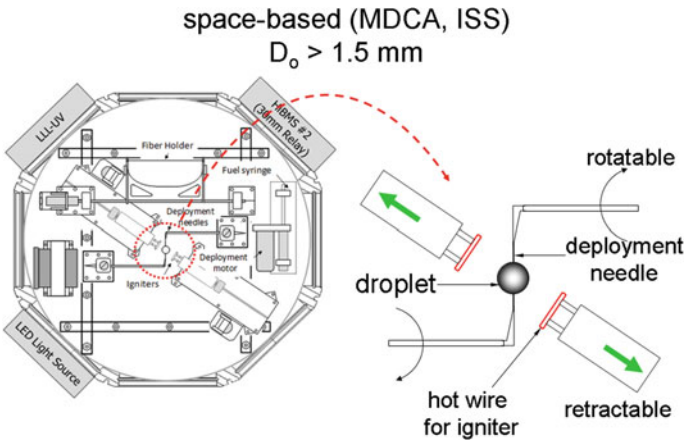

Fig. 6 Droplet deployment design for the multi-user droplet combustion facility (MDCA) (Dietrich et al. 2014; Robbins and Shinn 2010; Banu 2008). Droplet deployment is in microgravity by rapid retraction of two deployment needles to separate the droplet from the needles

Test droplets are ignited by hot wires on support tubes that are linearly retracted to provide an unobstructed ambience for burning. Hardware on the MDCA is adjusted through communication links from the ISS to a control center at NASA Glenn and through video and audio feeds to the author's laboratory at Cornell (Fig. 7). The MDCA also has the capability for supporting a test droplet onto an 80-μm-diameter fiber.

For a fiber-supported droplet, there is always a concern that the fiber will influence the droplet burning history. The effects involved can be distortion of the droplet shape (e.g., by surface tension effects), an influence on heat transfer to the droplet through the fiber, and/or inducing an asymmetric flow field in the surrounding gas. It was shown (Liu et al. 2014b) that for the design of Fig. 5 which incorporates a fiber of approximately 14 μm diameter and D_o < 0.6 mm, the influence of a fiber on burning is minimal and the droplet behaves as essentially as if it were free-floating when burning in the standard atmosphere, which is the environment in which this particular method has been used. The influence of a fiber on the gas phase flow field is revealed by using soot aggregates formed during the burning process as essentially particles that seed the flow. For droplets supported by a single fiber, rather unusual flow patterns can occur that are significantly different from the idealization of Fig. 4b and c (Avedisian and Jackson 2000).

For large droplets, Fig. 8 shows the gas motion that can be induced by the 80-μm fiber employed on the MDCA design (Liu et al. 2014b).

Interestingly, it was found that the onset of the motions shown in Fig. 8 coincided with a significant increase in the droplet burning rate as shown in Fig. 9. Nonetheless, regardless of the droplet and fiber diameters for any supported droplet design, an influence of the fiber will always be expected as the droplet evaporates because the droplet diameter decreases while the fiber diameter is fixed.

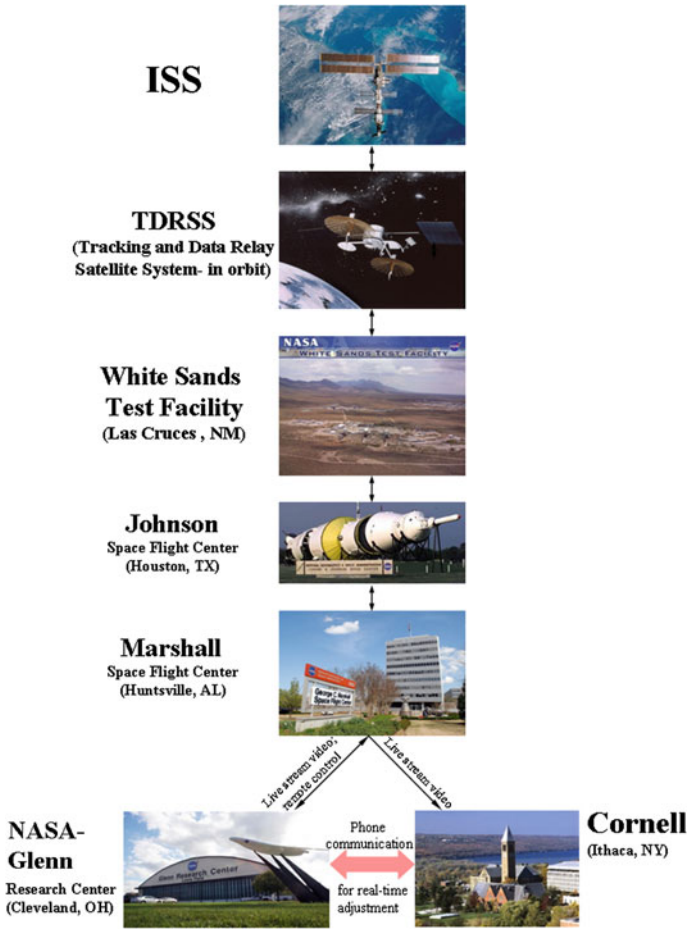

Fig. 7 Communication network for controlling operations on the MDCA. Hardware controls originate from NASA Glenn

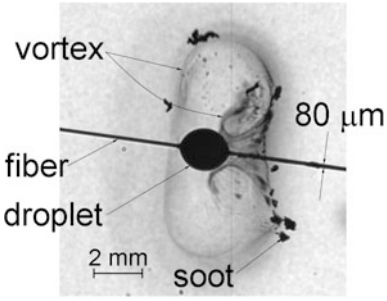

Fig. 8 Photograph of a fiber-supported n-decane droplet an n-decane droplet with D_o = 1.82 mm at t/D_o^2 = 0.4 s/mm^2 after ignition. Soot aggregates reveal a vortex-like motion adjacent to the fiber (Liu et al. 2014a)

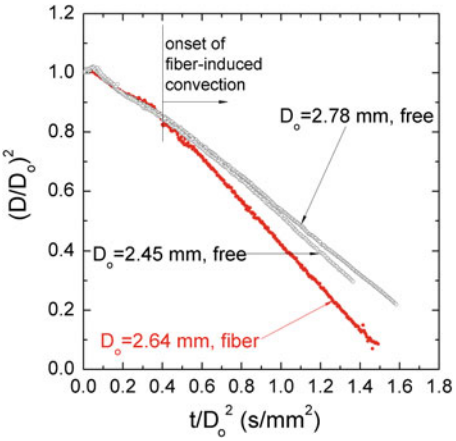

Fig. 9 Evolution of "large" droplet diameters of the indicated initial values showing the effect of an 80-μm support fiber using the experimental design of Fig. 6 on the ISS (Liu et al. 2014b). The ratio of droplet diameter of the fiber is large enough for no influence of a fiber to have been anticipated. The clear deviation of the burning rate of the fiber-supported droplet from the free droplet is attributed to the onset of convection and the *vortical motions* shown in Fig. 8

5 Visualization of the Droplet Burning Process

The main diagnostic for the droplet burning experiments discussed here is photographic. Figure 10 shows the burning history of a backlighted unsupported n-heptane droplet that illustrates development of the soot shell for D_o = 0.76 mm (Jackson and Avedisian 1998). The flame is not visible in this sequence as is typical

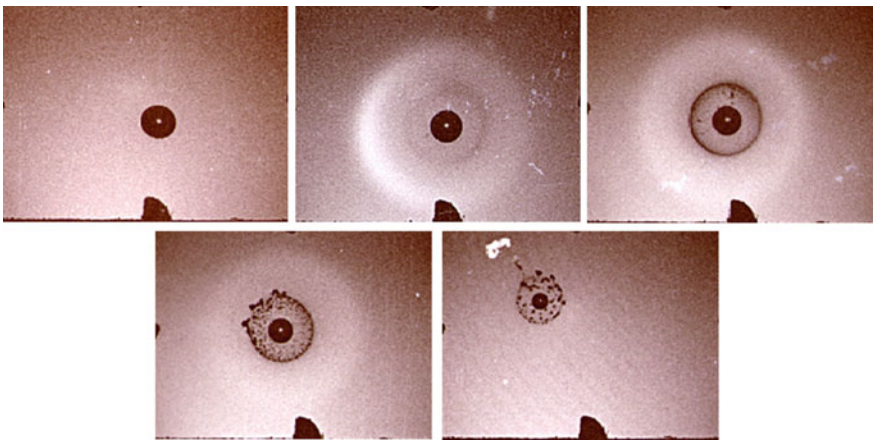

Fig. 10 Selected images from an unsupported droplet burning sequence for n-heptane (D_o = 0.76 mm) showing development of the soot shell (Jackson and Avedisian 1998). Flame is also visible in this sequence. Camera marker on the film is at the bottom of the photographs

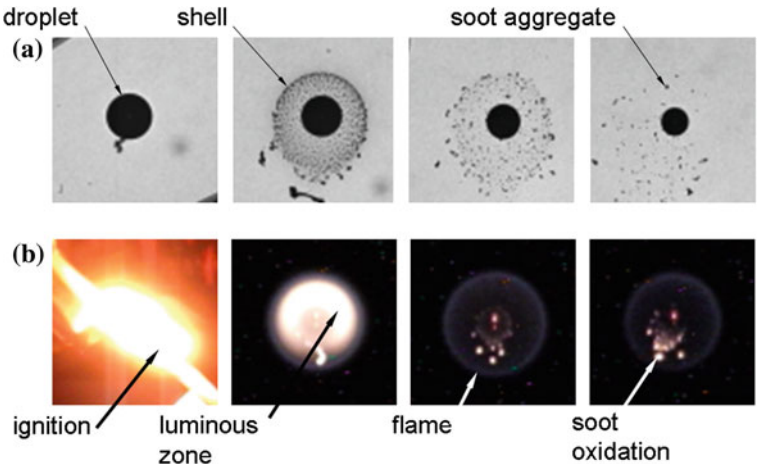

Fig. 11 Selected photographs from the burning history of a D_o = 2.78 mm n-octane droplet showing backlighted images (**a**) and development of the sooting dynamics, and flame-illuminated images (**b**) showing development of the flame (Liu et al. 2014b)

of backlighting. Figure 11 displays backlighted images of an unsupported large n-octane droplet (D_o = 2.78 mm Liu et al. 2014a) from ISS experimentation, as well as a flame-illuminated sequence (Fig. 11b) of the same droplet (i.e., no backlighting is used). The soot shell is again clearly visible as are individual aggregates that formed.

When developing a surrogate, qualitative comparisons of the flame luminosity can provide a clue about the efficacy of the surrogate. Figure 12 compares the flame luminosity for several small hydrocarbon droplets considered as surrogate constituents for an octane 87 gasoline (heptane, octane, toluene, and iso-octane).

The images are arranged according to their 'brightness' (i.e., the sensitivity of the eye to wavelengths in the visible region of the electromagnetic spectrum due to oxidation and incandescence of soot aggregates that are transported to the flame). The image brightness qualitatively correlates with the amount of soot formed, being greater with increasing soot formation.

Based on a qualitative assessment of the image brightness in Fig. 12, the sooting propensities (highest to lowest) consistent with Fig. 6 would be toluene > heptane/toluene > gasoline > iso-octane > heptane/iso-octane > heptane. The backlighted images show the intensity of the soot shell and are consistent with this approximate ordering. It could be concluded that if matching sooting propensity were an important consideration in developing a surrogate for gasoline, neither heptane, iso-octane, or their mixtures would work. Toluene, on the other hand, has a noticeably brighter flame than gasoline. As such, one could envision that blending toluene with heptane or iso-octane would produce a feasible surrogate for gasoline, at least in terms of sooting propensities.

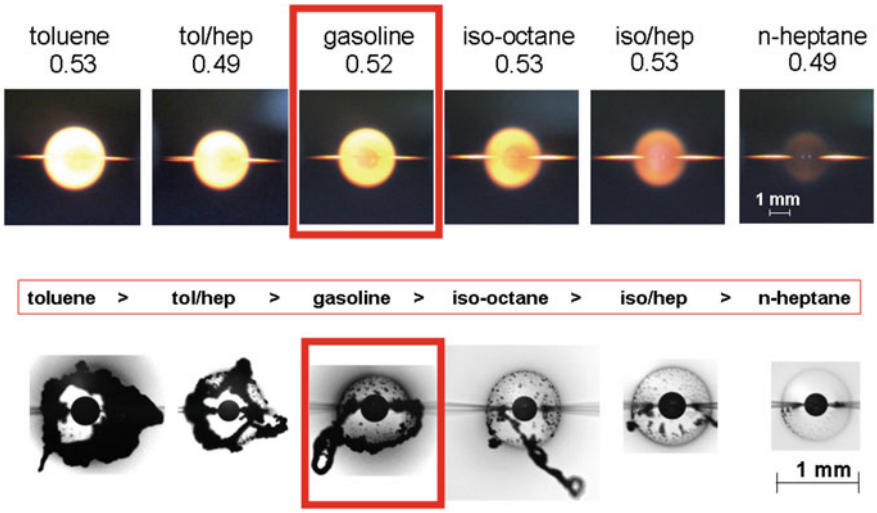

Fig. 12 *Upper row* of images are taken from self-illuminated color videos, arranged from highest to lowest intensity. Numbers denote the initial droplet diameters in mm. The images were selected from each sequence for maximum qualitative luminosity. *Lower row* of images are backlighted video that show soot dynamics; the images were selected for the thickest soot cloud in the burning sequence. The indicated sooting trend is based on a qualitative assessment of the flame image intensity (Liu and Avedisian 2012). The *red box* is a reference for gasoline

For sufficiently large D_o, the flame will extinguish owing to radiation (Chao et al. 1990). The flame diameter becomes so large that the flame temperature drops below that needed to sustain the combustion process. Figure 13 shows an example of the dynamics of this process for an n-decane droplet studied in the MDCA where an oscillatory behavior is noted. The mechanism for this process is not fully understood, though it may be related to droplet size and motion.

As burning progresses, the droplet diameter decreases and the flame is reduced perhaps for chemical kinetic reasons. Continued reduction of temperature will extinguish the flame. When the droplet moves (even slightly), it enters a fresh oxidizing ambience on the front side, while on the back side, the gas is depleted of oxygen. The flame is then hottest on the front, while on the opposite side, it is colder and extinction can occur locally as manifested by a hole appearing in the flame that propagates around the droplet as oxygen is used up. As the extinction boundary moves to the front of the droplet, it enters a region of gradually enriched oxygen concentration and higher temperature due to the flow and the flame recedes to the back side as combustion is re-established, thereby completing one cycle of an oscillation. This sort of oscillatory phenomenon has often been associated with "cool flame" phenomena (Nayagam et al. 2012; Farouk and Dryer 2013; Dietrich et al. 2014).

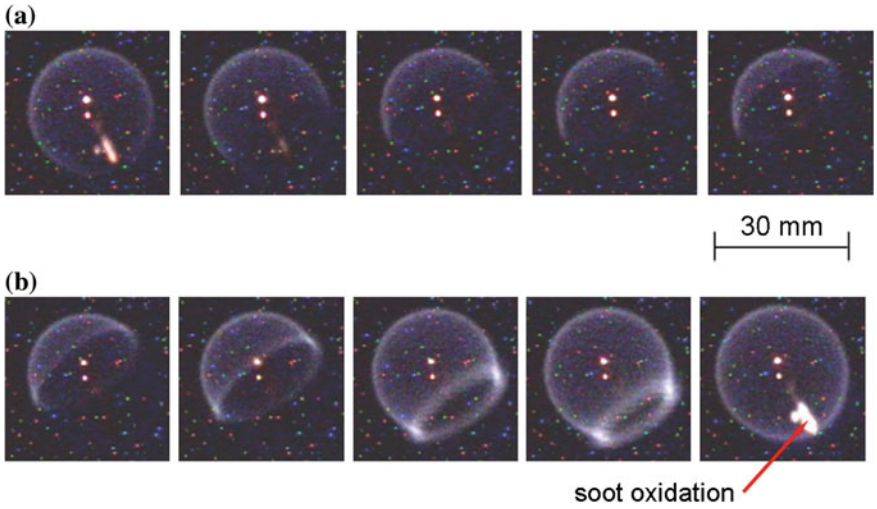

Fig. 13 Self-illuminated images showing oscillations of a n-decane droplet flame ($D_o = 5.1$ mm) as it radiatively extinguishes (Liu et al. 2014a). Time between images is 0.17 s. Flame peels away from the droplet (the droplet is not visible in these flame images) and then closes around the droplet as the flame is re-established. Specks in background are from video sensor imperfections. (Also see this website, http://www.smithsonianmag.com/science-nature/zero-g-fire-pulses-jellyfish-space-station-180952454/). **a** Flame opens-up. **b** Flame closes-back

6 Combustion Properties of the Spherical Droplet Flame Configuration

As remarked previously and depicted in Fig. 4, the combustion properties for the spherical droplet flame are the droplet diameter (D), the flame diameter (D_f), and the soot shell diameter (D_s). These dimensions are obtained by a frame-by-frame analysis of the digital video record of the droplet burning history. Computer-based algorithms have been developed for this purpose (Dembia et al. 2012). The droplet diameter is relatively easy to measure while the flame, and especially the soot shell diameter, can be challenging and time-consuming to extract from images like those shown in Fig. 11 because the flame and soot shell boundaries are not especially distinct. As such, the effort to extract droplet dimensions can be quite arduous, especially if soot obscures part of the droplet boundary which can create gaps in the measurements. The following illustrates results of using combustion properties obtained from the experimental designs of Figs. 5 and 6 to assess performance of surrogates.

To be effective, a surrogate should replicate the combustion properties of the real fuel in a suitable combustion configuration. Arguments have been previously presented for the suitability of the spherical droplet flame configuration to serve that purpose. Using the evolution of droplet diameter as a combustion property for the spherical flame configuration (Fig. 4), Fig. 14 compares an 87 octane gasoline (no ethanol) with toluene and mixtures of heptane and toluene. A binary mixture is the

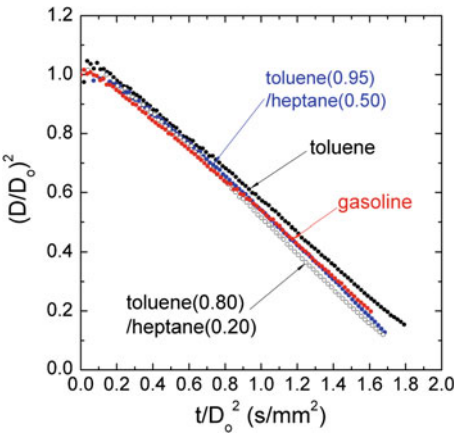

Fig. 14 Comparison of the evolution of droplet diameter of gasoline with toluene and mixtures of toluene with heptane (Liu et al. 2012). The closest match with gasoline is for 5 % heptane in toluene

simplest blend for a surrogate. Varying the composition is a relatively simple task for a binary system, and optimization techniques are not needed to identify the composition that produces the best match of combustion properties between the surrogate and real fuel.

Heptane and iso-octane were found to have essentially the same droplet burning characteristics for the configuration of Fig. 4. Figure 14 shows that neither heptane (nor iso-octane since heptane and iso-octane burn in an almost identical manner (Liu et al. 2012) can replicate the evolution of droplet diameter, which is consistent with the less luminous flames of heptane and iso-octane compared to gasoline.

Toluene droplet flames are, however, more luminous than gasoline (Fig. 12). As such, from a mixing perspective, blending toluene with heptane (or iso-octane, for that matter) can result in sooting propensities that are closer to gasoline. Furthermore, because toluene burns slower than gasoline while heptane burns faster as shown in Fig. 14, it will be possible to identify a heptane mixture fraction of heptane and toluene that closely matches the evolution of droplet diameter of gasoline. Figure 14 shows that a toluene/heptane mixture containing 5 % heptane and 95 % toluene accomplishes this quite well.

It is important to note that a surrogate may not be able to replicate all combustion properties of a real fuel. Considering the data in Fig. 15 which show the relative position of the flame to the droplet, gasoline droplet flames are much closer to the droplet surface than are toluene or heptane flames. A binary mixture evidently does not have enough flexibility to match more than a few combustion properties (one in this case). Including more constituents in a surrogate provides more flexibility to match combustion properties of a surrogate with a real fuel. Jet fuel surrogates (Dooley et al. 2010, 2012) are a case in point.

Two surrogates were formulated for jet-A: one containing three components (3CS) and the other four components (4CS). The surrogates were developed around four targets (average molecular weight (MW), DCN, TSI, and hydrocarbon-to-carbon ratio (H/C)) and the mixture fraction of the three or four components determined by

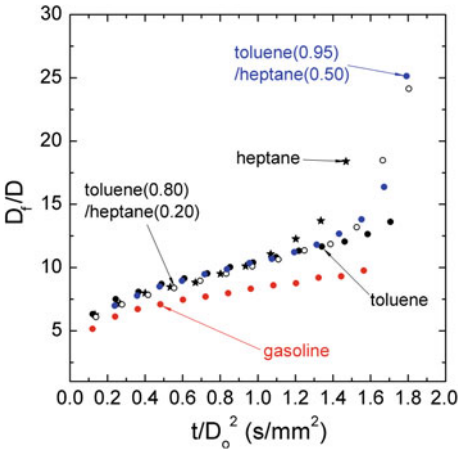

Fig. 15 Comparison of flame standoff ratio of gasoline with toluene and mixtures of toluene and heptane (Liu et al. 2012). The gasoline droplet flame is consistently closer to the droplet than for toluene or heptane/toluene mixture droplets, as contrasted with the closer match of the evolution of droplet diameter for a toluene/heptane mixture with gasoline shown in Fig. 14

an optimization algorithm. Table 3 lists the properties of the surrogates and the mixture fractions of the components. The 3CS surrogate matched only the DCN and H/C ratio, but not the TSI or MW. The 4CS surrogate was able to match the four targets. A test of these surrogates for the configuration of Fig. 4 was reported by Liu et al. (2013b). Figure 16 shows the results.

It is evident from Fig. 16 that the 3CS and 4CS blends represent jet-A quite well, with the 4CS being slightly better. This better agreement may be attributed to the fact that the 4CS matched four targets, while the 3CS, only two. Moreover, the relative position of the flame to the droplet for the 4CS was in slightly better agreement with jet-A than the 3CS as shown in Fig. 17, though as for that both surrogates were reasonably well correlated with jet-A.

As remarked previously, one of the more attractive features of the spherical droplet flame configuration of Fig. 4a is its one-dimensional gas transport that facilitates developing a numerical simulation of the burning process that can include detailed combustion chemistry, unsteady effects, and spectral radiative sub-models. Armed with this capability, it is possible to use measured combustion properties to evaluate some of the numerical inputs required for predictions [e.g., modifying the combustion chemistry to provide a better match between predicted and measured combustion properties (e.g., Werler et al. 2014)]. To illustrate the sort of comparative process that lies at the heart of using a detailed numerical simulation to predict combustion properties for the spherically symmetric droplet flame configuration, we consider methyl decanoate (MD) droplets burning under conditions that promote spherical droplet flames. MD is sometimes considered a surrogate for biodiesel derived from rapeseed oil as the feedstock.

Table 3 Representative properties and compositions of the three (3CS) and four (4CS) component surrogates of Dooley et al. (2010, 2012)

Fuel	Pure component	Formula	Density[a] (g/cm^3)	MW (g/mole)	BP (K)	Molar ratio[c]	Volume fraction (%)
3CS	n-decane	$C_{10}H_{22}$	0.726	142.28	443.7	0.427	50.86
	iso-octane	C_8H_{18}	0.688	144.23	372.4	0.33	33.34
	toluene	C_7H_8	0.862	92.14	383.8	0.243	15.80
4CS	n-dodecane	$C_{12}H_{26}$	0.745	170.33	489.5	0.40	50.36
	iso-octane	C_8H_{18}	0.688	144.23	372.4	0.29	26.67
	1,3,5-trimethylbenzene	C_9H_{12}	0.861	120.19	437.9	0.07	5.54
	Propylbenzene	C_9H_{12}	0.858	120.19	432.4	0.23	17.43
Jet-A	–	$C_{10.17}H^c_{19.91}$	0.800	142.01[c]	478–573[b]	–	–

[a] Measured using a digital density meter (Mettler Todelo DA-100M) at 24.6 °C
[b] Colket et al. (2007)
[c] Dooley et al. (2010, 2012)

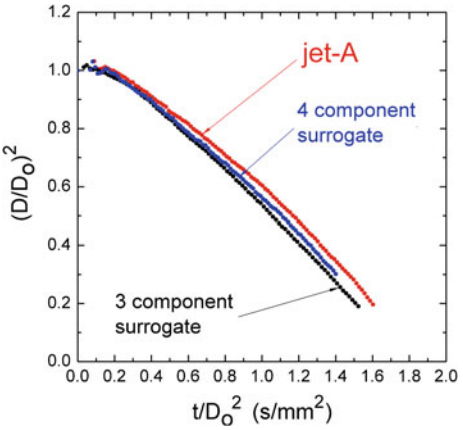

Fig. 16 Comparison of the evolution of droplet diameter for a 3CS and 4CS (Table 3) with jet-A (Liu et al. 2013b)

A recent study (Liu et al. 2013a) showed the efficacy of a detailed numerical simulation of the configuration of Fig. 4a to predict combustion properties of MD using the kinetic scheme of Divart et al. (2012). The reaction kinetics incorporated 238 species and 1,244 reaction mechanisms. As such, the simulation solved 238 individual species conservation equations simultaneously along with detailed formulations for radiative transfer, physical property correlations, and unsteady heat transfer in the droplet and surrounding gas.

Figures 18 and 19 compare measured droplet diameters and relative positions of the droplet to the flame with predicted values. The experimental method (cf. Fig. 5) employed droplets suspended from SiC fibers. As the fiber thermal conductivity was not known, values of 5.2, and 0 W/mK (a free droplet) were employed in the computation.

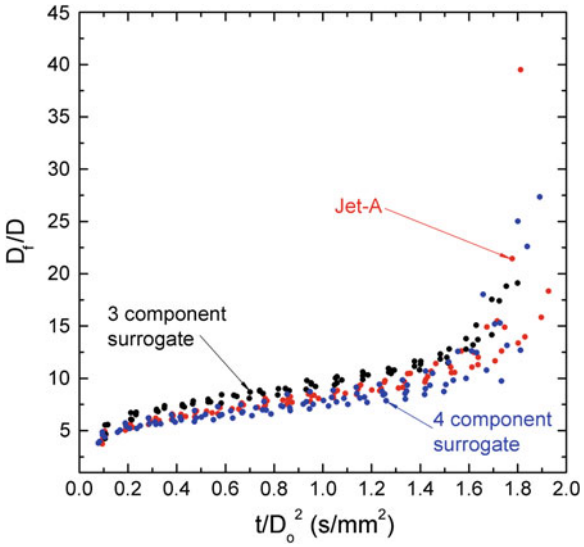

Fig. 17 Evolution of the measured relative position of the flame to the droplet for the 3CS and 4CS (Liu et al. 2013b in comparison with the flame position of jet-A

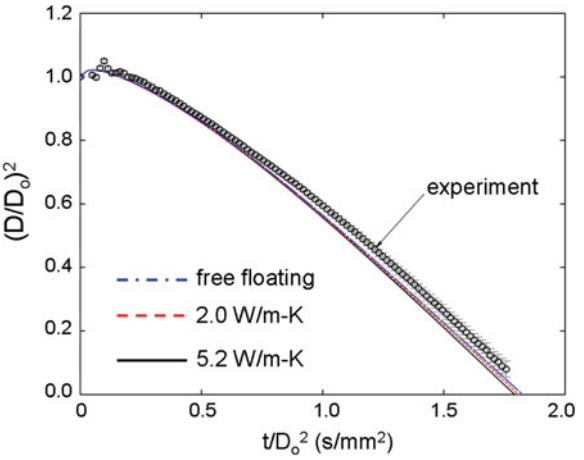

Fig. 18 Comparison of the measured evolution of droplet diameter for a methyl decanoate droplet with a detailed numerical simulation (*solid line*) of the spherically symmetric droplet burning process. The droplets were supported by a SiC fiber (Fig. 5), and predictions for various fiber thermal conductivities are shown (from Liu et al. 2013a)

The agreement between simulated and measured combustion properties for MD is very good as shown in Figs. 18 and 19. This agreement is testimony to the relevance of the Dievart et al. (2012) kinetic mechanism for MD. It is this sort of comparative analysis that lies at the heart of evaluating the inputs needed to

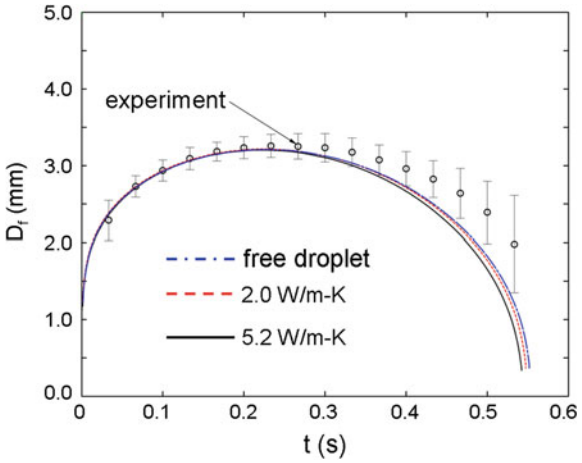

Fig. 19 Comparison of the measured evolution of flame (or outer luminous zone) diameter for a methyl decanoate droplet with a detailed numerical simulation (*solid lines*). Data are for the same droplet as Fig. 18. The droplets were supported by a SiC fiber (Fig. 5), and predictions for various fiber thermal conductivities are shown (from Liu et al. 2013a)

simulate more complex combustion configurations. Armed with this information, detailed modeling can then be used to determine with some confidence the operational conditions under which the formation of gas products responsible for degrading fuel efficiency can be minimized, thus increasing fuel efficiency of combustion engines.

7 Summary and Conclusions

The development of surrogates for liquid transportation fuels is one of the most important problems that will impact the ability to predict in-cylinder processes of combustion engines using detailed numerical simulation. Real fuels are so complex that it is not currently possible to develop kinetic and property database inputs needed to simulate engine performance. Surrogates are the only viable way to address this problem.

The traditional approach to assessing the performance of surrogate fuels has been to use low-dimensional combustion configurations that require the liquid to be pre-vaporized. This restriction eliminates from consideration the performance of a surrogate when multiphase processes are important such as spray injection which sets the initial conditions for in-cylinder combustion processes. The combustion of an isolated droplet burning with spherically symmetric gas phase transport provides a platform that folds into the assessment of a liquid surrogate some of the basic evaporation and phase equilibrium dynamics of sprays, while at the same time providing a transport process that is amenable to detailed numerical modeling.

Results were summarized that illustrate the efficacy of the spherical flame configuration to provide combustion properties useful for assessing the performance of surrogate fuels. Though it will not generally be possible to match all combustion properties of a combustion configuration used in the development of a surrogate fuel, the current capabilities show that complex transportation fuels can benefit from including combustion properties obtained from the spherical flame configuration in assessing the performance of surrogate fuels.

Acknowledgments Preparation of this paper was supported in part by the National Aeronautics and Space Administration grant no. NNX08AI51G with Mr. Michael Hicks as the project monitor. The author also benefitted from discussions with Dr. Y.C Liu of the University of Michigan-Flint and Mr. Yuhao Xu of Cornell University. The author is pleased to acknowledge this essential help in the course of his work on droplet combustion processes.

References

Amsden AA (1999) KIVA-3V, Release 2, Improvements to KIVA-3V, Los Alamos National Laboratory, report LA-UR-99-915

Avedisian CT (1997) Soot formation in spherically symmetric droplet combustion. In: Physical and chemical aspects of combustion, Chap. 6. Gordon and Breach, New York pp 135–160

Avedisian CT (2008) Surrogate fuel development: the role of droplet burning. Paper no. IMECE2008-68748, proceedings of IMECE2008, ASME international mechanical engineering congress and exposition, Boston, Massachusetts, Oct 31–Nov 6 2008

Avedisian CT, Callahan BJ (2000) Combustion of nonane/hexanol mixture droplets in microgravity. Proc Combust Inst 28:991–997

Avedisian CT, Jackson GS (2000) Soot patterns around suspended n-heptane droplet flames in a convection-free environment. J Propul Power 16:974–979

Avedisian CT, Yang JC, Wang CH (1988) On low gravity droplet combustion. Proc Roy Soc Lond A420:183–200

Banu B (2008) Fluids and combustion facility (FCF) and combustion integrated rack (CIR). Payload Accommodations Handbook CIR-DOC-4064, NASA John H, Glenn Research Center, Cleveland, Ohio

Bieleveld T, Frassoldati A, Cuoci A, Faravelli T, Ranzi E, Niemann U (2009) Experimental and kinetic modeling study of combustion of gasoline, its surrogates and components in laminar non-premixed flows. Proc Combust Inst 32:493–500

Chao BH, Law CK, T'ien JS (1990) Structure and extinction of diffusion flames with flame radiation, extinction of diffusion flames with flame radiation. Proc Combust Inst 23:523–531

Chaos M, Zhao Z, Kazakov A, Gokulakrishnan P, Angioletti M, Dryer FL (2007) A PRF+ toluene surrogate fuel model for simulating gasoline kinetics. Paper no. E26, 5th US National combustion meeting, Western States Section, Combustion Institute, 25–28 Mar 2007

Choi BC, Choi SK, Chung SH (2011) Soot formation characteristics of gasoline surrogate fuels in counterflow diffusion flames. Proc Combust Inst 33:609–616

Colket M, Edwards T, Williams S, Cernansky NP, Miller DL, Egolfopoulos F, Linstedt P, Seshadri K, Dryer FL, Law CK, Friend D, Lenhert DB, Pitsch H, Sarofim A, Smooke M, Tsang W (2007) Development of an experimental database and kinetic models for surrogate jet fuels. Paper no. AIAA2007-770, 45th aerospace sciences meeting, Reno, 8–11 Jan 2007

Cuoci A, Mehl M, Buzzi-Ferraris G, Faravelli T, Manca D, Ranzi E (2005) Autoignition and burning rates of fuel droplets under microgravity. Combust Flame 143(2005):221–226

Dagaut P, Togbe C (2008) Oxidation kinetics of butanol–gasoline surrogate mixtures in a jet-stirred reactor: Experimental and modeling study. Fuel 87:3313–3321

Dembia CL, Liu YC, Avedisian CT (2012) Automated data analysis of consecutive digital images from droplet combustion experiments by a MATAB-based algorithm. Image Anal Stereology 31:137–148

Dietrich DL, Nayagam V, Hicks MC, Ferkul PV, Dryer FL, Farouk T, Shaw BD, Suh HK, Choi MY, Liu YC, Avedisian CT, Williams FA (2014) Droplet combustion experiments aboard the International Space Station. Microgravity Sci Technol. doi:10.1007/s12217-014-9372-2 (open access)

Dievart P, Won SH, Dooley S, Dryler FL, Ju Y (2012) A kinetic model for methyl decanoate combustion. Combust Flame 159:1793–1805

Dirks LC, Dirks GW, Wu J (2012) Evolving perspectives on biofuels in the United States. Front Energy 6:379–393

Dooley S, Won SH, Chaos M, Heyne J, Ju Y, Dryer FL, Kumar K, Sung CJ, Wang H, Oehlschlaeger MA, Santoro RJ, Litzinger TA (2010) A jet fuel surrogate formulated by real fuel properties. Combust Flame 157:2333–2339

Dooley S, Won SH, Jahangirian SJUY, JU Y, Dryer FL, Wang H, Oehlschlaeger MA (2012) The combustion kinetics of a synthetic paraffinic jet aviation fuel and a fundamentally formulated experimentally validated surrogate fuel. Combust Flame 159:3014–3020

Edwards T, Maurice LQ (2001) Surrogate mixtures to represent complex aviation and rocket fuels. J Propul Power 17:461–466

Fahd EA, Liu YC, Avedisian CT, Dryer FL, Farouk TI (2014) A detailed numerical simulation of spherically symmetric n-butanol droplet combustion and comparisons with experimental data. Proceedings of the Combustion Institute, vol 35 (in press)

Farouk T, Dryer FL (2013) Isolated alkane droplet combustion in microgravity: cool flames. Paper no.: 1G17, 8th U.S. National combustion meeting, Combustion Institute, Park City, Utah, 19–22 May 2013

Farouk TI, Liu YC, Avedisian CT, Dryer FL (2013) Sub-millimeter sized methyl butanoate droplet combustion: Microgravity experiments and detailed numerical modeling. Proc Combust Inst 34:1609–1616

Farrell JT, Cernansky NP, Dryer FL, Friend DG, Hergart CA, Law CK, McDavid RM, Mueller CJ, Patel AK, Pitsch H (2007) Development of an experimental database and kinetic models for surrogate diesel fuels. SAE paper no. 2007-01-0201

FR (2012) Federal Register, National Archives and Records Administration, vol 77(199), pp 62623–63200, 15 Oct 2012

Gauthier BM, Davidson DF, Hanson RK (2004) Shock tube determination of ignition delay times in full-blend surrogate fuel mixtures. Combust Flame 139:300–311

Hara H, Kumagai S (1990) Experimental investigation of free droplet combustion under microgravity. Proc Combust Inst 23:1605–1610

Huber ML, Lemmon EW, Bruno TJ (2010) Surrogate mixture models for the thermophysical properties of aviation fuel Jet-A. Energy Fuels 24:3565–3571

Jackson GS, Avedisian CT (1998) Combustion of unsupported water-in-heptane emulsion droplets in a convection-free environment. Int J Heat Mass Transf 41:2503–2515

Jackson GS, Avedisian CT, Yang JC (1991) Soot formation during combustion of unsupported methanol/toluene mixture droplets in microgravity. Proc Roy Soc Lond A435:359–368

Lee CH, Reitz RD (2013) A comparative study on CFD simulation of spray penetration between gas jet and standard KIVA-3V spray model over a wide range of ambient gas densities. J Mech Sci Technol 26:4014–4025

Lee Y, Jang K, Han K, Huh KY (2013) Simulation of a heavy duty diesel engine fueled with soybean biodiesel blends in low temperature combustion. SAE paper no. 2013-01-1100

Liu YC, Avedisian CT (2012) A comparison of the burning characteristics of sub-millimeter droplets of binary mixtures of iso-octane, n-heptane and toluene with a commercial unleaded gasoline. Combust Flame 159:770–783

Liu YC, Farouk TI, Savas AJ, Dryer FL (2013a) On the spherically symmetrical combustion of methyl decanoate droplets and comparisons with detailed numerical modeling. Combust Flame 160:641–655

Liu YC, Savas AJ, Avedisian CT (2013b) Spherically symmetric droplet combustion of three and four component miscible mixtures as surrogates for Jet-A. Proc Combust Inst 34:1569–1576

Liu YC, Rah JK, Trenou KN, Hicks MC, Avedisian CT (2014a) Experimental study of initial diameter effects on convection-free droplet combustion in the standard atmosphere for n-heptane, n-octane and n-decane: International Space Station and ground-based experiments. Paper no. AIAA-2014-1019, 52nd aerospace sciences meeting, National Harbor, Md., 13–17 Jan 2014

Liu YC, Xu Y, Hicks MC (2014b) The role of micro-convection induced by support fiber in droplet Combustion processes. Proceedings of the Combustion Institute, vol 35 (in press)

Mueller CJ, Cannella WJ, Bruno TJ, Bunting B, Dettman HD, Franz JA, Huber ML, Natarajan M, Pitz WJ, Ratcliff MA (2012) Methodology for formulating diesel surrogate fuels with accurate compositional, ignition-quality, and volatility characteristics. Energy Fuels 26:3284–3303

Narayanaswamy K, Pepiot P, Pitsch H (2013) Jet fuels and Fischer-Tropsch fuels: surrogate definition and chemical kinetic modeling. Paper # 070RK-0273, Western States section meeting, Combustion Institute, 19–22 May 2013

Nayagam V, Dietrich DL, Ferkul PV, Hicks MC, Williams FA (2012) Can cool flames support quasi-steady alkane droplet burning? Combust Flame 159:3583–3588

NSF (2011) Transforming combustion research through cyberinfrastructure. Committee on Building Cyberinfrastructure for Combustion Research, National Research Council, The National Academies Press. ISBN-13: 978-0-309-16387-3, April (http://www.nap.edu/catalog.php?record_id=13049)

Okajima S, Kumagai S (1975) Further investigations of combustion of free droplets in a freely falling chamber including moving droplets. Proc Combust Inst 15:401–407

Pitz WJ, Mueller CJ (2011) Recent progress in the development of diesel surrogate fuels. Prog Energy Combust Sci 37:330–350

Pitz JW, Cernansky NP, Dryer FL, Egolfopoulos FN, Farrell JT, Friend DG, Pitsch H (2007) Development of an experimental database and chemical kinetic models for surrogate gasoline fuels. SAE paper no. 2007-01-0175

PRECISE (2011) U.S. Department of Energy, Office of Energy Efficiency and Renewable Energy and Science, March 3. http://www1.eere.energy.gov/vehiclesandfuels/pdfs/presice_rpt.pdf

Robbins J, Shinn C (2010) Multi-user droplet combustion apparatus FLEX-2. Reflight Safety Data Package MDC-DOC-1790A, NASA John H. Glenn Research Center, Cleveland, Ohio

Sirignano WA (1999) Fluid dynamics and transport of droplets and sprays. Cambridge University Press, Cambridge

Tsang W (2003) Workshop on combustion simulation databases for real transportation fuels, report no. NISTIR 7155, National Institute of Standard and Technology, Gaithersburg, MD, 4–5 Sept 2003

USEIA (2014) U.S. Energy Information Administration, Independent Statistics and Analysis. March. http://www.eia.gov/forecasts/steo/pdf/uncertainty.pdf

Wang H, Reitz JD, Yao M, Yang B, Jiao Q, Qiu L (2013) Development of an n-heptane-n-butanol PAH mechanism and its application for combustion and soot production. Combust Flame 160:504–519

Werler M, Cancino LR, Schiessl R, Mass U, Schulz C, Fikri M (2014) Ignition delay times of diethyl ether measured in a high-pressure shock tube and a rapid compression machine. Proceedings of the Combustion Institute, vol 35 (in press)

Yahyaoui M, Djeballi-Chaumeix N, Dagaut P, Paillard CE, Gail S (2007) Experimental and modeling study of gasoline surrogate mixtures oxidation in jet stirred reactor and shock tube. Proc Combust Inst 31:385–391

Zhang HR, Eddings EG, Sarofim AD (2007) Criteria for selection of components for surrogates of natural gas and transportation fuels. Proc Combust Inst 31:401–409